Direct spectroscopic observation of a shallow hydrogen-like donor state in insulating $SrTiO_3$

Z. Salman,[1,*] T. Prokscha,[1,†] A. Amato,[1] E. Morenzoni,[1] R. Scheuermann,[1] K. Sedlak,[1] and A. Suter[1]

[1] *Paul Scherrer Institute, Laboratory for Muon Spin Spectroscopy, CH-5232 Villigen PSI, Switzerland*

(Dated: September 22, 2014)

We present a direct spectroscopic observation of a shallow hydrogen-like muonium state in $SrTiO_3$ which confirms the theoretical prediction that interstitial hydrogen may act as a shallow donor in this material. The formation of this muonium state is temperature dependent and appears below $\sim$ 70 K. From the temperature dependence we estimate an activation energy of $\sim$ 50 meV in the bulk and $\sim$ 23 meV near the free surface. The field and directional dependence of the muonium precession frequencies further supports the shallow impurity state with a rare example of a fully anisotropic hyperfine tensor. From these measurements we determine the strength of the hyperfine interaction and propose that the muon occupies an interstitial site near the face of the oxygen octahedron in $SrTiO_3$. The observed shallow donor state provides new insight for tailoring the electronic and optical properties of $SrTiO_3$-based oxide interface systems.

arXiv:1409.5534v1 [cond-mat.mtrl-sci] 19 Sep 2014

The discovery of a high mobility two-dimensional electron gas (2DEG) at the interface between two insulating Perovskite oxides; TiO_2-terminated $SrTiO_3$ (STO) and $LaAlO_3$ (LAO)[1–3] has prompted great interest in these oxides. In addition to the 2DEG, this interface was found to be magnetic[4–6] and even superconducting below $\sim$ 300 mK[7]. It is generally agreed that the high carrier densities at the interface are associated with various effects, including doping with electrons or oxygen vacancies [2, 8–11], inter-diffusion [10, 12, 13], and the influence of lattice distortions [14–18]. These discoveries provide an interesting prospect for producing interfaces with physical properties not present, nor predictable, from the constituent materials, and may lead to new technological applications. Here we discuss the response of these oxides to impurities, in particular hydrogen, which may play an important role in the discovered phenomena. Moreover, we note that the reported results are extremely relevant for possible applications of STO and related insulating oxides in fuel cells and hydrogen sensors [19–21].

Hydrogen is an ubiquitous impurity in device or sample fabrication and can cause unintended modifications of the electronic and structural properties. For example, the properties of the 2DEG at STO/LAO interfaces may be affected if additional free charge carriers are present due to unintentional doping [22]. The electronic behaviour of interstitial hydrogen can be characterized by the position of the H(+/-) level in the band gap, where the formation energies of H^+ and H^- are equal. If this level is close to or intersecting the conduction/valence band, hydrogen will act as a shallow donor/acceptor. In elemental and binary semiconductors, a universal alignment of the H(+/-) level at $\sim$ -4.5 eV with respect to the vacuum level has been found theoretically [23] and supported by experiments [24]. The model predicted successfully hydrogen shallow donor states in ZnO and InN [25–27]. In this model the H(+/-) level coincides approximately with the host's charge neutrality level (CNL). In general the CNL is found to be located at relatively constant energies with respect to the vacuum level [23, 28]. The coincidence of the H(+/-) level with the CNL can be understood as follows. In a binary semiconductor H^+ and H^- behave similarly, i.e. they break a bond at the anion or cation site, respectively, leaving a dangling bond at the opposite cation or anion site. The H(+/-) level is then located midway in between the energy levels of the dangling bonds, which corresponds to the CNL.

In oxides the situation is different, since H^+ tends to form an OH^- antibonding state, without breaking a cation–O bond. H^-, on the other hand, causes the formation of an oxygen dangling bond by breaking a metal–O bond. Thus, the H(+/-) level is determined by the average of the oxygen dangling bond and OH^- antibonding levels, which is located at relatively constant energies of about $4.5 - 5.5$ eV above the valence band maximum [28, 29]. Therefore, hydrogen should form a shallow donor state in oxides with a band gap of less than $\sim$ 4.5 eV, such as STO which has an indirect band gap of $\sim$ 3.2 eV. This prediction has been supported recently by a new theoretical work on hydrogenated vacancies and hidden hydrogen in STO [30]. In contrast, the universal alignment model described above places H(+/-) deep in the band gap, i.e. $\sim$ 0.5 eV below the conduction band minimum, which equals the electron affinity of STO and is located at about 4.0 eV below the vacuum level. Note, the model in Refs. [28, 29] predicts shallow donor states in SnO_2, TiO_2, ZrO_2, and HfO_2 which have been observed or inferred in muon spin rotation (μSR) experiments [31]. In these experiments, positive muons, when implanted into insulators or semiconductors, can capture an electron to form interstitial muonium [Mu=(μ^+e^-)], which can be considered as a light hydrogen isotope and mimics its chemical and electrical interactions. In fact, a large amount of information on the structure and electrical activity of isolated interstitial H states in semiconductors and insulators has been obtained by Mu spectroscopy [32, 33].

In this Letter we present a direct spectroscopic ob-

servation of a shallow hydrogen-like Mu state in a STO (100) single crystal, in agreement with the model suggested by Refs. [28, 29]. Our results are consistent with muons occupying an interstitial site in the lattice, between two O–O bonds near the face of the oxygen octahedron. We find that up to $\sim 60\%$ of the implanted muons form a shallow muonium state at 25 K with a relatively small hyperfine coupling. From the field dependence of the Mu characteristic precession frequencies we find that the hyperfine tensor is fully anisotropic and estimate the hyperfine interaction along the principal axes of the tensor $A_X = 1.4 \pm 0.1$ MHz, $A_Y = 6.7 \pm 0.1$ MHz and $A_Z = 11.5 \pm 0.1$ MHz. This Mu state is one of the rare clear examples of a fully anisotropic Mu.

The μSR experiments were performed on the DOLLY, GPS and LEM spectrometers at the Paul Scherrer Institut in Villigen, Switzerland. In these experiments 100% polarized positive muons are implanted into the sample. Each implanted muon decays (lifetime $\tau_\mu = 2.2$ μs) emitting a positron preferentially in the direction of its polarization at the time of decay. Using appropriately positioned detectors, one measures the asymmetry of the muon beta decay along different directions as a function of time, $A(t)$, which is proportional to the time evolution of the muon spin polarization. $A(t)$ depends on the electronic environment of the muon and is used to extract information on the hyperfine interaction between the muon and the electrons in the system. Muonium is spectroscopically identified by its characteristic precession frequencies which allow to determine the Mu hyperfine parameters [32, 33]. In a low energy μSR (LE-μSR) experiment, the energy of the implanted muons, E, can be tuned (1-30 keV) to perform a measurement of $A(t)$ at depths in the range $\sim 1 - 200$ nm [34, 35]. The measurements reported here were performed on a $15 \times 15 \times 1$ mm single side epitaxially polished (100) STO single crystal substrate (Crystal GmbH). In the bulk μSR measurements, the sample was suspended on an aluminized Mylar tape and mounted into a He gas flow cryostat. The muons were implanted with their polarization nominally along $\langle 100 \rangle$ with the field applied perpendicular to it (nominally along $\langle 010 \rangle$). In the LE-μSR measurements the sample was glued to a cold finger cryostat, with the field applied along $\langle 100 \rangle$ and the polarization of implanted muons perpendicular to it.

We start by looking at muon spin precession measurements in a field of $B = 10$ mT applied perpendicular to the muon's initial spin direction. At room temperature we find that all muons implanted at 4.1 MeV in bulk STO precess at the Larmor frequency of μ^+, $\nu_0 = \gamma_\mu/2\pi\ B$, with almost no damping. Here, $\gamma_\mu/2\pi = 135.5$ MHz/T is the muon gyromagnetic ratio. As we decrease the temperature, we find that below ~ 70 K the amplitude of the signal precessing at ν_0 (the so called diamagnetic fraction, f_{μ^+}) decreases sharply, reaches a minimum at ~ 30 K, and then increase at lower temperatures (Fig. 1). Similar behaviour is observed at lower muon implantation energies. However, in this case the decrease in the f_{μ^+} is smaller, and at $E = 1.6$ keV we observe no increase at low temperatures.

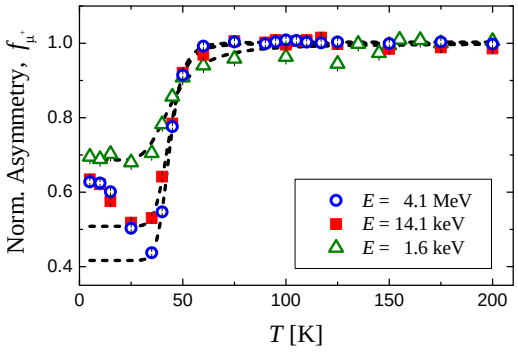

FIG. 1: (Color online) The normalized diamagnetic fraction of the μ^+ precession signal at $B = 10$ mT as a function of temperature. Circles, squares and triangles are measurements at 4.1 MeV ($B \perp \langle 100 \rangle$), 14.1 keV and 1.6 keV ($B \parallel \langle 100 \rangle$), respectively. The drop in asymmetry below ~ 70 K is due to formation of muonium. The dashed lines are fits to Eq. 1.

Closer investigation of the measured asymmetries in the bulk below 70 K reveals that the polarization contains additional components with precession frequencies higher than ν_0. Example asymmetries, measured at 25 K and applied fields of 1 and 10 mT are shown in Fig. 2(a). Note that the additional frequencies are of the order of few MHz [see Fig. 2(b)], which we attribute to Mu precession frequencies. These are directly related to the hyperfine interaction of Mu and confirm its formation at these temperatures. The size of these frequencies (< 10 MHz) indicates that a "shallow" Mu state is formed, i.e. much

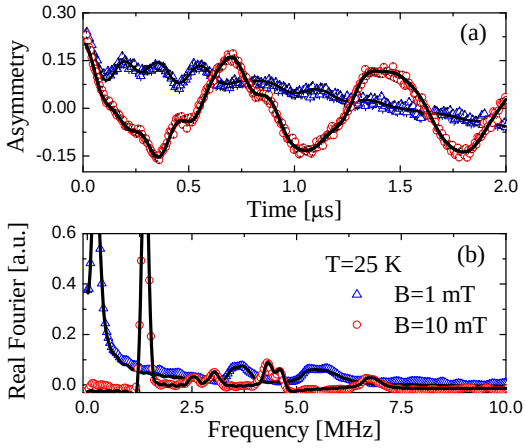

FIG. 2: (Color online) (a) The asymmetries at $T = 25$ K as a function of time for applied fields 1 and 10 mT ($B \perp \langle 100 \rangle$) and (b) the corresponding real Fourier transform showing at least four muonium precession frequencies in both cases. The solid lines are fits to a sum of precessing and damping signals.

smaller than the ~ 4.4 GHz frequency observed for vacuum Mu.

The temperature dependence of f_{μ^+} is related to the Mu fraction, $f_{\rm Mu} = 1 - f_{\mu^+}$. It can be calculated following a semi-empirical model [31],

$$f_{\mu^+} = 1 - f_{\rm Mu} = 1 - \frac{f_0}{1 + N\exp(-\Delta/T)}, \qquad (1)$$

where f_0 is the normalized maximum Mu fraction, N is a density-of-states parameter and Δ is the Mu activation energy which can be considered as an effective ionization or binding energy [31]. A fit of f_{μ^+} in bulk (circles in Fig. 1), between 25 and 200 K, yields an ionization energy of $\Delta = 600 \pm 15$ K or 52 ± 2 meV. Similar fits for the data at low implantation energies yield $\Delta = 515 \pm 15$ K (45 ± 2 meV) and 270 ± 10 K (23 ± 1 meV) for 14.1 keV and 1.6 keV, respectively. Similar decrease in shallow muonium ionization energy near the surface has been recently detected in ZnO and CdS. This effect is attributed to the presence of electric fields due to band bending near the free surface [36].

It is worthwhile noting here that the absence of (or weak) energy dependence of the diamagnetic fraction below ~ 10 K indicates that the Mu formation at low T does not depend on the number of track electrons, i.e., there is no *delayed* Mu formation below $T \sim 10$ K. Mu can form in two ways: i) *promptly* during charge-exchange collisions with subsequent thermalization as neutral Mu, and ii), *delayed*, where the positive muon thermalizes at an interstitial lattice site, followed by a capture of an electron from its own ionization track. The latter is significantly suppressed if the number of track electrons is $\lesssim 10^3$, corresponding to implantation energies of less than a few keV [37]. It is also suppressed in materials with a large dielectric constant, ε, where the electric field of the muon point charge is effectively screened by the surrounding medium, thus suppressing the probability of capturing a track electron. In STO, $\varepsilon \sim 300$ at room temperature, reaches ~ 10000 at ~ 25 K and then saturates at $20000 - 25000$ below 10 K [38]. The increase of the diamagnetic fraction below ~ 30 K in the bulk may be due to the increasing ε at these temperatures, as *delayed* Mu formation becomes less likely. The low temperature flattening of f_{μ^+} corresponds well to the saturation of ε.

It is somewhat surprising that a shallow Mu state can be observed in a system with such a large ε. For shallow donors, one usually applies a hydrogenic effective-mass model to estimate the binding energy of the donor to be $E_D \sim R_y(m^*/m_e)/\varepsilon^2$, where $R_y = 13.6$ eV the Rydberg constant , m_e the electron mass, and m^* the conduction-band effective mass of the electron [31]. This approximation is justified by the large electron wave-function spreading over several lattice sites. This implies that at 25 K, where $\varepsilon \sim 10000$ in STO, the binding energy should be zero, i.e. no Mu should form. Therefore, the observation of a shallow Mu state indicates that it might have a more localized polaronic character [31]. Furthermore, it is known that doping of STO may increase m^*/m_e up to ~ 20 [39], and that an electric field may lower ε [40]. Hence, "doping" STO with Mu may cause a local deformation of the lattice with a local modification of m^* and ε.

Now we turn to evaluating the hyperfine interaction tensor of Mu. We consider a general Hamiltonian for a muon (spin $\mathbf{I}$) interacting with an electron (spin $\mathbf{S}$) with a fully anisotropic hyperfine interaction [41],

$$\mathcal{H} = \gamma_e B S_z - \gamma_\mu B I_z + A_Z S_Z I_Z + A_Y S_Y I_Y + A_X S_X I_X. \qquad (2)$$

where γ_μ and γ_e are the muon and electron gyromagnetic ratios, z is defined by the direction of B and A_i ($i = X, Y, Z$) are the Mu hyperfine interactions along the principal axes. The coordinates $(X, Y, Z)/(x, y, z)$ denote

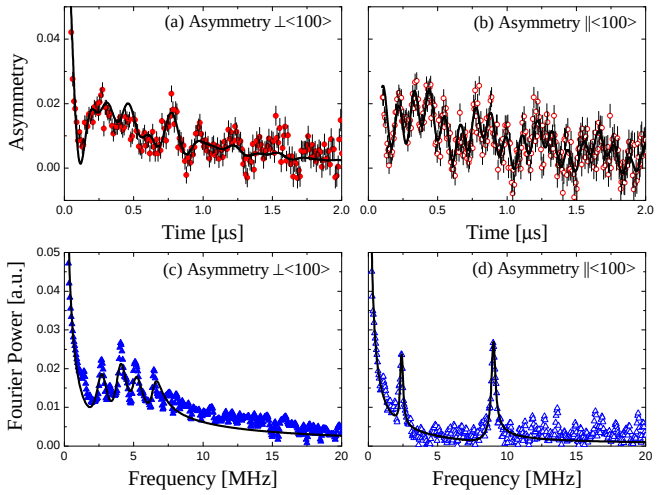

FIG. 3: (Color online) The asymmetries measured (a) parallel and (b) perpendicular to $\langle 100 \rangle$ at $T = 25$ K and in ZF. (c) and (d) are the corresponding Fourier transform showing clear ZF muonium precession frequencies in both cases. The solid lines are fits to a sum of precessing and damping signals

the hyperfine interaction/laboratory frame, such that the components of a spin angular momentum vector seen in the (X, Y, Z) system are expressed in terms of the components of the same vector seen in the (x, y, z) system as

$$\begin{bmatrix} S_X \\ S_Y \\ S_Z \end{bmatrix} = D(\alpha, \beta, \gamma) \begin{bmatrix} S_x \\ S_y \\ S_z \end{bmatrix}, \qquad (3)$$

where α, β,and γ are the Euler angles of the three consecutive rotations around Z, Y, and Z axes of the (X, Y, Z) coordinate system, which initially coincides with the (x, y, z) system. In ZF, the Hamiltonian (2) can be diagonalized analytically to calculate the Mu frequencies, giving a maximum of 6 possible frequencies depending on the values of A_i [41]. These are the sums and differences

of the different A_i parameters. Indeed our ZF measurement, shown in Fig. 3(a) and (b), with different relative orientations between the implanted muon spin and STO crystal give $\nu = 2.4, 2.7, 4.1, 5.1, 6.5$ and 9 MHz [Fig. 3(c) and (d)]. From these we estimate the hyperfine parameters $A_X = 1.4 \pm 0.1$ MHz, $A_Y = 6.7 \pm 0.1$ MHz and $A_Z = 11.5 \pm 0.1$ MHz.

Next, we extract the field dependent Mu precession frequencies from the asymmetries measured in bulk STO at 25 K. Here, we limit ourselves to four/five most visible frequencies for each field, as plotted in Fig. 4. Using

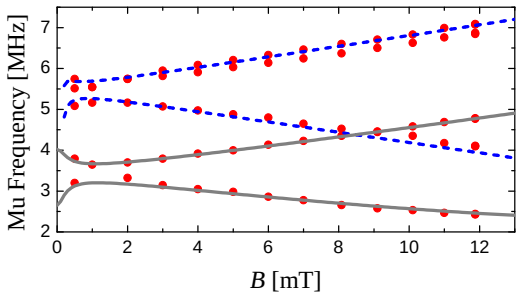

FIG. 4: (Color online) The observed Muonium precession frequencies as a function of applied field (with an angle of $\sim 14°$ between B and $\langle 010 \rangle$) at $T = 25$K. The lines are calculated values with $A_X = 1.37$, $A_Y = 6.67$ and $A_Z = 11.52$ MHz with $(\alpha, \beta, \gamma) = (0°, 57°, 27°)$ (solid) and $(0°, 17°, 0°)$ (dashed).

A_i values we calculate the Mu frequencies in an applied field by numerical diagonalization of $\mathcal{H}$. The amplitudes or probabilities of precession between different Mu energy states depend on the initial spin direction of the muon relative to the hyperfine principal axes. We find that in order to best model the field dependence in Fig. 4, one has to set the $(\alpha, \beta, \gamma) = (0°, 57°, 27°)$ (solid line in Fig. 4) and $(0°, 17°, 0° \pm 45°)$ (dashed line in Fig. 4). The agreement with our experimental results is excellent considering the uncertainties and limited resolution in the experimental data. Note, there is a small frequency splitting in the highest frequency branch. This may be attributed to a small amount of mosaicity or the structural distortion in STO at this temperature [42]. Such effect results in different domain orientations and thus a small variation in the local environment of Mu, which can only be resolved at high frequencies. Using the extracted hyperfine parameter to calculate the precessing amplitudes reveals that there is no missing fraction, i.e., $f_{\mu^+} + f^{\mathrm{S}}_{\mathrm{Mu}} = 1$, where $f^{\mathrm{S}}_{\mathrm{Mu}}$ is the fraction of shallow Mu. This excludes the existence of any Mu state deep in the band gap. Although we cannot exclude that the observed neutral muonium centre is metastable, the fact that the summ of the Mu^+ and Mu^0 fractions accounts for the full muon polarization, suggests an equilibrium balance between the two charge states. The observed hyperfine interaction strength and ionization energy imply a shallow donor state, modelling the analogous hydrogen state [43].

Note that the angle between the STO cubic axes and the normal to the face of the oxygen octahedron are $\sim 54°$. Therefore, the hyperfine tensor and the first set of angles (solid lines in Fig. 4) could be attributed to a Mu occupying an interstitial site between two O–O bonds and near the face of the oxygen octahedron in the STO crystal. The determination of the second set of angles (dashed lines in Fig. 4) is much less reliable since it shows a much weaker angular dependence. Nevertheless, if we assume that the angle between the applied field and the $\langle 010 \rangle$ is $\sim 14°$, then these angles are also consistent with the same Mu site. Our results are consistent with neutron diffraction results [44], infrared absorption experiments and theoretical studies on hydrogen defect vibrational modes [45, 46] as well as other theoretical work [30]. However, they disagree with Refs. [47–50] which place the hydrogen on O–O bond or the face of the cube between corner sharing Sr atoms and the O atoms at the face center. Note also that such sites, which have high symmetry, will result in an axially symmetric Mu hyperfine tensor. Surprisingly, we also find that the implanted muons occupy a different site from that occupied by other implanted impurities in STO such as Li [51, 52].

In conclusion, we present a direct spectroscopic observation of a shallow hydrogen-like muonium state in STO. This confirms a theoretical prediction that interstitial hydrogen may act as a shallow donor in STO [28–30]. The formation of this muonium state appears below ~ 70 K and implies an activation energy of ~ 50 meV in bulk which decrease to ~ 25 meV near the surface of the crystal. We find that the shallow impurity state has a fully anisotropic hyperfine tensor, with $A_X = 1.4 \pm 0.1$ MHz, $A_Y = 6.7 \pm 0.1$ MHz and $A_Z = 11.5 \pm 0.1$ MHz. These results provide strong evidence of the sensitivity of the electronic properties of STO, and in particular its surface region, to impurities. Finally, since hydrogen is an ubiquitous impurity, these findings may prove crucial for interpretation of the variety of observed phenomena at LAO/STO interfaces [1–3]. We believe that hydrogen doping effect may be a possible explanation for the excess charge carriers at the interfaces of LAO/STO, and therefore require a more detailed experimental and theoretical consideration. We propose that a systematic study of the transport properties of LAO/STO interfaces as a function of hydrogen doping may provide quantitative information about this effect.

This work was performed at the Swiss Muon Source (SμS), Paul Scherrer Institute (PSI, Switzerland). We would like to thank Rob Kiefl, Kim Chow and João Campos Gil for useful suggestions and fruitful discussions. We are also grateful to Ekaterina Pomjakushina for her assistance with the allignment of the crystals.

* Electronic address: zaher.salman@psi.ch
† Electronic address: thomas.prokscha@psi.ch

[1] A. Ohtomo and H. Y. Hwang, Nature **427**, 423 (2004).
[2] S. Thiel, G. Hammerl, A. Schmehl, C. W. Schneider, and J. Mannhart, Science **313**, 1942 (2006).
[3] M. Huijben, G. Rijnders, D. H. A. Blank, S. Bals, S. V. Aert, J. Verbeeck, G. V. Tendeloo, A. Brinkman, and H. Hilgenkamp, Nat. Mater. **5**, 556 (2006).
[4] A. Brinkman, M. Huijben, M. V. Zalk, J. Huijben, U. Zeitler, J. C. Maan, G. V. der Wiel, G. Rijnders, D. H. A. Blank, and H. Hilgenkamp, Nat. Mater. **6**, 493 (2007).
[5] M. Ben Shalom, C. W. Tai, Y. Lereah, M. Sachs, E. Levy, D. Rakhmilevitch, A. Palevski, and Y. Dagan, Phys. Rev. B **80**, 140403(R) (2009).
[6] Z. Salman, O. Ofer, M. Radovic, H. Hao, M. Ben Shalom, K. H. Chow, Y. Dagan, M. D. Hossain, C. D. P. Levy, W. A. MacFarlane, et al., Phys. Rev. Lett. **109**, 257207 (2012).
[7] N. Reyren, S. Thiel, A. D. Caviglia, L. F. Kourkoutis, G. Hammerl, C. Richter, C. W. Schneider, T. Kopp, A.-S. Ruetschi, D. Jaccard, et al., Science **317**, 1196 (2007).
[8] R. Pentcheva and W. E. Pickett, Phys. Rev. B **74**, 035112 (2006).
[9] M. S. Park, S. H. Rhim, and A. J. Freeman, Phys. Rev. B **74**, 205416 (2006).
[10] M. Takizawa, H. Wadati, K. Tanaka, M. Hashimoto, T. Yoshida, A. Fujimori, A. Chikamatsu, H. Kumigashira, M. Oshima, K. Shibuya, et al., Phys. Rev. Lett. **97**, 057601 (2006).
[11] A. Kalabukhov, R. Gunnarsson, J. Borjesson, E. Olsson, T. Claeson, and D. Winkler, Phys. Rev. B **75**, 121404 (2007).
[12] N. Nakagawa, H. Y. Hwang, and D. A. Muller, Nat. Mater. **5**, 204 (2006).
[13] P. R. Willmott, S. A. Pauli, R. Herger, C. M. Schlepütz, D. Martoccia, B. D. Patterson, B. Delley, R. Clarke, D. Kumah, C. Cionca, et al., Phys. Rev. Lett. **99**, 155502 (2007).
[14] C. H. Ahn, J.-M. Triscone, and J. Mannhart, Nature **424**, 1015 (2003).
[15] S. Gemming and G. Seifert, Acta Mater. **54**, 4299 (2006).
[16] D. R. Hamann, D. A. Muller, and H. Y. Hwang, Phys. Rev. B **73**, 195403 (2006).
[17] J.-L. Maurice, C. Carrétéro, M.-J. Casanove, K. Bouzehouane, S. Guyard, E. Larquet, and J.-P. Contour, Phys. Status Solidi (a) **203**, 2209 (2006).
[18] S. Okamoto, A. J. Millis, and N. A. Spaldin, Phys. Rev. Lett. **97**, 056802 (2006).
[19] T. Higuchi, T. Tsukamoto, K. Kobayashi, S. Yamaguchi, Y. Ishiwata, N. Sata, K. Hiramoto, M. Ishigame, and S. Shin, Phys. Rev. B **65**, 033201 (2001).
[20] T. Higuchi, T. Tsukamoto, N. Sata, M. Ishigame, Y. Tezuka, and S. Shin, Phys. Rev. B **57**, 6978 (1998).
[21] H. Yukawa, K. Nakatsuka, and M. Morinaga, Solid State Ionics **116**, 89 (1999).
[22] W.-j. Son, E. Cho, J. Lee, and S. Han, J. Phys.: Condens. Matter **22**, 315501 (2010).
[23] C. G. Van de Walle and J. Neugebauer, Nature **423**, 626 (2003).
[24] R. L. Lichti, K. H. Chow, and S. F. J. Cox, Phys. Rev. Lett. **101**, 136403 (2008).
[25] S. F. J. Cox, E. A. Davis, S. P. Cottrell, P. J. C. King, J. S. Lord, J. M. Gil, H. V. Alberto, R. C. Vilão, J. Piroto Duarte, N. Ayres de Campos, et al., Phys. Rev. Lett. **86**, 2601 (2001).
[26] D. M. Hofmann, A. Hofstaetter, F. Leiter, H. Zhou, F. Henecker, B. K. Meyer, S. B. Orlinskii, J. Schmidt, and P. G. Baranov, Phys. Rev. Lett. **88**, 045504 (2002).
[27] E. A. Davis, S. F. J. Cox, R. L. Lichti, and C. G. Van de Walle, Appl. Phys. Lett. **82**, 592 (2003).
[28] K. Xiong, J. Robertson, and S. J. Clark, J. Appl. Phys. **102**, 083710 (2007).
[29] P. W. Peacock and J. Robertson, Appl. Phys. Lett. **83**, 2025 (2003).
[30] J. B. Varley, A. Janotti, and C. G. Van de Walle, Phys. Rev. B **89**, 075202 (2014).
[31] S. F. J. Cox, J. L. Gavartin, J. S. Lord, S. P. Cottrell, J. M. Gil, H. V. Alberto, J. P. Duarte, R. C. Vilão, N. A. d. Campos, D. J. Keeble, et al., J. Phys. Cond. Mat. **18**, 1079 (2006).
[32] B. D. Patterson, Rev. Mod. Phys. **60**, 69 (1988).
[33] A. Yaouanc and P. D. de Réotier, *Muon Spin Rotation, Relaxation, and Resonance: Applications to Condensed Matter* (OUP Oxford, 2010).
[34] E. Morenzoni, R. Khasanov, H. Luetkens, T. Prokscha, A. Suter, N. Garifianov, H. Gluckler, M. Birke, E. Forgan, H. Keller, et al., Physica B **326**, 196 (2003).
[35] T. Prokscha, E. Morenzoni, K. Deiters, F. Foroughi, D. George, R. Kobler, A. Suter, and V. Vrankovic, Nucl. Instr. and Meth. A **595**, 317 (2008).
[36] T. Prokscha, H. Luetkens, E. Morenzoni, G. J. Nieuwenhuys, A. Suter, M. Döbeli, M. Horisberger, and E. Pomjakushina, arXiv:1408.6972 [cond-mat] (2014), arXiv: 1408.6972.
[37] T. Prokscha, E. Morenzoni, D. G. Eshchenko, N. Garifianov, H. Gluckler, R. Khasanov, H. Luetkens, and A. Suter, Phys. Rev. Lett. **98**, 227401 (2007).
[38] K. A. Müller and H. Burkard, Phys. Rev. B **19**, 3593 (1979).
[39] J. Ravichandran, W. Siemons, M. L. Scullin, S. Mukerjee, M. Huijben, J. E. Moore, A. Majumdar, and R. Ramesh, Phys. Rev. B **83**, 035101 (2011).
[40] S. Hyun and K. Char, Appl. Phys. Lett. **79**, 254 (2001).
[41] M. Senba, Physical Review A **62**, 042505 (2000).
[42] R. Cowley, Phil. Trans. R. Soc. London A **354**, 2799 (1996).
[43] S. F. J. Cox, Rep. Prog. in Phys. **72**, 116501 (2009).
[44] N. Sata, K. Hiramoto, M. Ishigame, S. Hosoya, N. Niimura, and S. Shin, Phys. Rev. B **54**, 15795 (1996).
[45] M. C. Tarun and M. D. McCluskey, J. Appl. Phys. **109**, 063706 (2011).
[46] J. T-Thienprasert, I. Fongkaew, D. J. Singh, M.-H. Du, and S. Limpijumnong, Phys. Rev. B **85**, 125205 (2012).
[47] G. Weber, S. Kapphan, and M. Wöhlecke, Phys. Rev. B **34**, 8406 (1986).
[48] D. Houde, Y. Lépine, C. Pépin, S. Jandl, and J. L. Brebner, Phys. Rev. B **35**, 4948 (1987).
[49] S. Klauer and M. Wöhlecke, Phys. Rev. Lett. **68**, 3212 (1992).
[50] L. Villamagua, R. Barreto, L. M. Prcel, and A. Stashans, Phys. Scr. **75**, 374 (2007).
[51] Z. Salman, E. P. Reynard, W. A. MacFarlane, K. H. Chow, J. Chakhalian, S. R. Kreitzman, S. Daviel, C. D. P. Levy, R. Poutissou, and R. F. Kiefl, Phys. Rev.

B **70**, 104404 (2004).
[52] Z. Salman, R. F. Kiefl, K. H. Chow, M. D. Hossain, T. A. Keeler, S. R. Kreitzman, C. D. P. Levy, R. I. Miller, T. J. Parolin, M. R. Pearson, et al., Phys. Rev. Lett. **96**, 147601 (2006).